Real Time Condition Monitoring Using Camera and Phase-Based Motion Estimation

SEUNGHWAN LEE, YINAN MIAO, YESEUL KONG, HYEONWOO NAM and GYUHAE PARK

ABSTRACT

Defects on manufacturing equipment, such as abrasion, corrosion, and deposition, may decrease the production quality and even lead to the shutdown of the entire manufacturing line. Various condition monitoring technologies have been developed to predict machine health and safety through contact sensors. The noncontact camera has shown many advantages over the conventional contact sensors, including high spatial resolution, low cost and remote sensing. Moreover, phase-based motion amplification has proven to be an efficient tool for detecting subtle vibrations. However, the motion amplification requires significant computational resources and does not provide direct motion signal output. To detect abnormal vibrationsduring long-term inspections, a more efficient phase-based motion estimation technique is necessary. In this study, we propose a real-time vibration monitoring system that uses a camera and image phase. We use single optimal Gabor filter with phase-based optical flow to extract the vibrational motion. The use of single optimal filter significantly reduces computation costs and enables accurate measurement of vibration signals even in the low-light condition and/or with image noise. Parallel computing scheme is also introduced for real-time condition monitoring. We conducted validation experiments on a structure with multiple vibrating components that simulate a real factory line. Damage detection is performed on the structure with two damaged cases. All the results show that the proposed technique can accurately measure displacement and provide a novel solution for camera-based real-time damage detection.

INTRODUCTION

Cameras have emerged as a powerful tool for monitoring the state of structures and mechanical systems. Compared to traditional contact sensors, cameras offer high-resolution measurements without mass loading effects and reduce costs by eliminating

Seunghwan Lee, Yinan Miao, Yeseul Kong, Hyeonwoo Nam, Gyuhae Park, Advanced Structures and Dynamics Laboratory (ASDL), Department of Mechanical Engineering, College of Engineering, Chonnam National University, Gwangju, Republic of Korea.

the need for installation of numerous physical sensors [1]. Seveal camera-based techniques have been developed for estimating motion. Digital image correlation enables full-field measurements and is applicable to three-dimensional deformation of structures[2-4]. Advanced Edge detection using wavelet transforms can measure the displacement with sub-pixel accuracy [5].

The concept of phase generation, using quadrature filters such as complex steerable filters and complex Gabor filters, is key in revealing subtle movements in images. One prominent technique for motion magnification, proposed by Wadhwa et al. [6], uses a complex steerable pyramid to achieve multi-scale and multi-direction image decomposition. This process involves targeting different spatial frequencies with a series of steerable filters, tracking phase changes over time, and then rescaling these to amplify motion at the targeted frequency band. Various studies have aimed to enhance the precision of camera-based techniques by leveraging motion magnification [7-9].

However, challenges remain, such as magnified noise, nonlinear phase, and computation costs, which may limit the application of these techniques in real-time monitoring tasks. To address these issues, we propose a real-time vibration monitoring system using phase-based optical flow with an optimal Gabor filter. This technique achieves accurate measurements even in the complex capturing environments. Additionally, we developed a parallel computing scheme optimized for phase-based real-time motion processing to reduce computational costs. Experimental validation on a structure simulating the real factory confirms the accuracy and robustness of the proposed technique, demonstrating its potential for real-time monitoring tasks.

THEORY AND METHOD

Phase-Based Displacement Measurement using Optimal Complex Gabor Filter

To measure displacement, the phase-based optical flow (POF) using a single optimal complex Gabor filter is adopted [10-11]. The filter's common form in the spatial domain is a 2D Gaussian envelope and a 2D complex sinusoid as shown:

$$G(x,y) = Ge(x,y) * (cos(2\pi(u_0 x + v_0 y)) + jsin(2\pi(u_0 x + v_0 y))) \quad (1)$$

where (u_0, v_0) is the center frequency, and $Ge(x,y)$ is the Gaussian envelope. When an image is filtered with the 2D complex Gabor filter, it becomes a complex-valued image matrix:

$$R(x,y) = A_{re}(x,y) + jA_{im}(x,y) \quad (2)$$

The phase is calculated as:

$$\varphi(x,y) = arctan2(A_{im}(x,y)/A_{re}(x,y)) \quad (3)$$

By assuming that the local phase contour remains constant in the image sequence, motion estimation is performed using differentiation of the spatial phase gradient:

$$(\varphi_x, \varphi_y, \varphi_t) \cdot (v_x, v_y, 1) = \sqrt{(\varphi_x^2 + \varphi_y^2)(v_x^2 + v_y^2)}\, cos(\beta) + \varphi_t = 0 \quad (4)$$

where (v_x, v_y) is a vector that represents the full velocity, (φ_x, φ_y) is the spatial phase gradient, β is the angle between phase gradient and full velocity, and φ_t is the phase change over time (after phase unwrapping).

The component velocity $\vec{v}_c$ is the projection of the full velocity on the direction of phase gradient, which can be calculated using Eq. 4,

$$\vec{v}_c = \vec{\varphi}^n_{x,y} \|\vec{v}_c\| = \frac{-\varphi_t}{(\varphi_x^2+\varphi_y^2)} (\varphi_x, \varphi_y) \tag{5}$$

Displacement of an object in a video is estimated by multiplying the velocity $(\vec{v}_c)$ components with the sampling interval of consecutive frames:

$$d(x, y, t) = \vec{v}_c(x, y, t) * \Delta t \tag{6}$$

The technique enables the measurement of small displacements on structures without the need for separate tracking markers or patterns. However, the phase can be unstable due to complex measurement environment, which may reduce the accuracy of measured displacement .

Research has been conducted to optimize the complex Gabor filter to address this issue [11-12]. The complex Gabor can be constructed in both spatial and frequency domains, as shown in Fig. 1. Three parameters control the shapes of the filter, center frequency (u_0, v_0), standard angular deviation (σ_a), and standard radial deviation (σ_r). The use of a single optimal complex Gabor filter not only eliminates the issue of unstable phase, but reduces the computation cost for real-time monitoring.

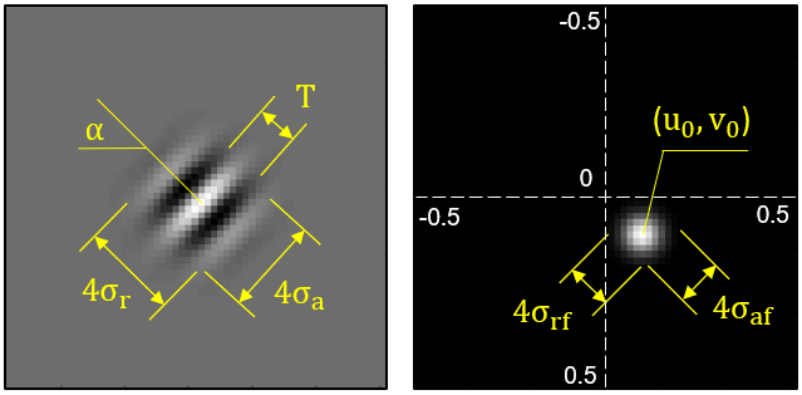

$T = 8$ pxl, $\alpha = 45°$, $(u_0, v_0) = (0.0884, 0.0884)$

$\sigma_r = 5$pxl, $\sigma_a = 5$ pxl, $\sigma_{rf} = 0.159$ pxl, $\sigma_{af} = 0.159$ pxl

Figure 1 Filter Parameters of 2D Complex Gabor filter

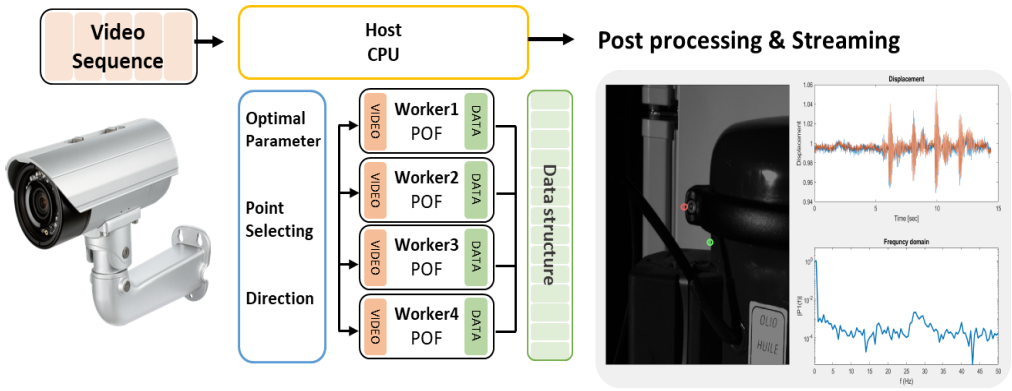

Figure 2 System flow of real-time monitoring system

Parallel Computing

The previous section discussed the technique with improved computational efficiency, but the processing time still needs to be improved for real-time monitoring at a rate of more than 200 frame per second. There are two methods to enhance the speed of image processing: utilizing CUDA and employing Multi-Core CPU [9]. The CUDA approach utilizes multiple general-purpose GPUs (Graphics Processing Units) for parallel processing, which significantly improves the speed of image processing. However, this method requires additional time for copying the image data to the GPU's memory.

The parallel processing scheme proposed in this study is optimized for phase-based technique using a complex Gabor filter and is based on Multi-Core CPU, as shown in Fig. 2. The Multi-Core CPU method utilizes the system memory and multiple CPU cores to accelerate image processing, providing a faster response even for memory allocation and deallocation of high-speed video data stream, which can involve data sizes of several tens of megabytes per second.

For processing in real-time, region of interest (100×100 pixels) was selected for each measuring points. Additionally, an ordered queue has been utilized to control the asynchronous situation between image capturing and POF computation.

EXPERIMENTAL VERIFICATION

Experimental Setup

As shown in Fig. 3, four component structures are installed on a plate that is excited by a shaker with an input of 36 Hz sinusoidal wave signal. Every component exhibits a local vibration under this excitation. The experiment uses a point-gray camera (FLIR BFS-U17S7M) with laptop (i9-12900H, 40GB ram). The camera is equipped with a ZEISS Milvus 2.8/15 lens, ensuring high-quality image capture at resolution of 640 x480. The frame rate is set at 250 frames per second.

The experiment data, which has seven labels, was obtained by monitoring the structure under two conditions : normal and damaged. Two types of damage, bolt loosening and pipe loosening, were simulated , as shown in Fig. 3c and TABLE I. The measurement points for the four components are marked, as shown in Fig. 3d.

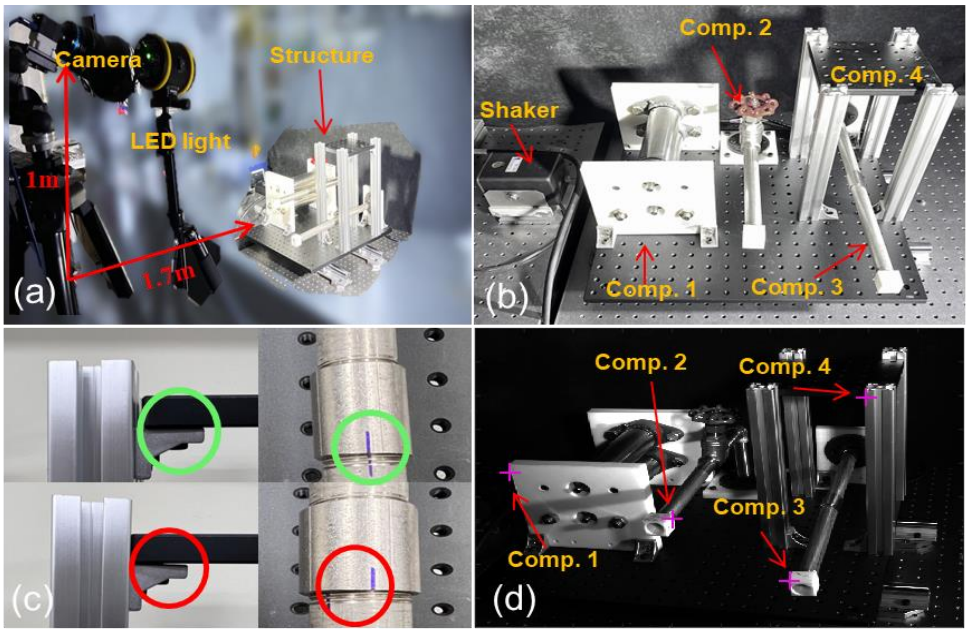

Figure 3 Validation experiment: a) experiment setup, b) shakers and the four component structures, c) damages (bolt loosening and pipe loosening), d) measuring points for each component

TABLE I. LABELING INFORMATION AND DATA OVERVIEW

Label	State	Location of defects	Number of data
#1	Normal	None	450
#2	Damaged	Comp. 3	75
#3	Damaged	Comp. 2	75
#4	Damaged	Comp. 1	75
#5	Damaged	Comp. 4	75
#6	Damaged	Comp.3-4	75
#7	Damaged	Comp.2-3	75

Structure	Label	Number of data (Normal/Damaged)
Comp.1	#1#4	450/75
Comp.2	#1 #3 #7	450/150
Comp.3	#1 #2 #6 #7	450/225
Comp.4	#1 #5 #6	450/150

The vibration signals were measured for 90 seconds in the normal state (#1) and 15 seconds for each with simulated damage (#2-7). The signals are divided into multiple 0.2-second samples (Normal state: 450 samples, damaged state: 75 samples for each).

Data Analysis

Figure 4 presents one of the measured datasets from Structure Component 3. the top row of the figure shows the data captured in the normal state (#1) and the damaged state (#6 and #7) from left to right. Time-frequency analysis was performed using discrete wavelet transform, which has better computational efficiency compared to short time Fourier transform. The resulting filtered data for different frequency bands are presented in rows 2 to 4 of Fig. 4.

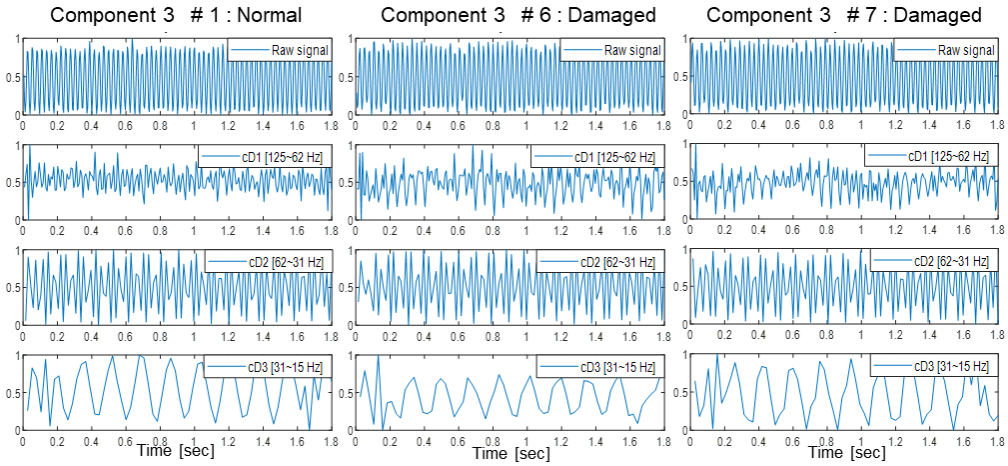

Figure 4 Time-frequency analysis using discrete wavelet transform

The feature extraction and dimensionality reduction algorithms were applied to cluster the measured data of all the structure components. The features were extracted in the time domain using detailed wavelet coefficients listed on the TABLE II. Principle component analysis was then carried out on these features, and the dimensionality reduction showed that the data were clustered according to the state of structure, as shown in Fig. 5 .

TABLE II. COMMONLY USED FEATURES IN CONDITION MONITORING FIELD

Features	Formula	Features	Formula	Features	Formula	Features	Formula
P1	$\frac{\sum_{n=1}^{N} x(n)}{N}$	P6	$\frac{\sum_{n=1}^{N} (x(n)-P1)^3}{(N-1)P2^3}$	P11	$\frac{\frac{1}{N}\sum_{n=1}^{N} x(n)^3}{\sigma^3}$	P16	$-\sum_{n=1}^{N} P(x)\ln P(x)$
P2	$\sqrt{\frac{\sum_{n=1}^{N} (x(n)-P1}{N-1}}$	P7	$\frac{\sum_{n=1}^{N} (x(n)-P1)^4}{(N-1)P2^4}$	P12	$\frac{\max(x)}{+\frac{\max(x)-\min(x)}{2(N-1)}}$	P17	$\frac{P4}{\frac{1}{N}\sum_{n=1}^{N} \lvert x(n)\rvert}$
P3	$\max\lvert x(n)\rvert$	P8	$\frac{P4^2}{\frac{1}{N}\sum_{n=1}^{N} \lvert x(n)\rvert}$	P13	$\frac{\min(x)}{-\frac{\max(x)-\min(x)}{2(N-1)}}$	P18	$\frac{P5}{\frac{1}{N}\sum_{n=1}^{N} \lvert x(n)\rvert}$
P4	$\sqrt{\frac{\sum_{n=1}^{N} (x(n))^2}{N}}$	P9	$\frac{P5^2}{\frac{1}{N}\sum_{n=1}^{N} \lvert x(n)\rvert}$	P14	$\frac{RMS}{Mean}$	P19	$\frac{\sum_{n=1}^{N} (x(n)-P1)^2}{N-1}$
P5	$\left(\frac{\sum_{n=1}^{N} \sqrt{\lvert x(n)\rvert}}{N}\right)^2$	P10	$\frac{\frac{1}{N}\sum_{n=1}^{N} x(n)^4}{\sigma^4}$	P15	$\frac{\max(x(n))}{RMS}$	P20	$\frac{\frac{1}{N}\sum_{n=1}^{N} \lvert x(n)\rvert}{N}$

TABLE III. FEATURES EXTRACTION BASSED ON WAVELET TRASNFORM

Features	Formula	Features	Formula	Features	Formula
W7	$\sqrt{\frac{\sum_{n=1}^{N} (Y(n))^2}{N-1}}$	W10	$\sqrt{\frac{\sum_{l=1}^{L} (Ryy(l))^2}{L-1}}$	W8	$\frac{W7}{\frac{1}{N}\sum_{n=1}^{N} \lvert Y(n)\rvert}$
W11	$E[\left(\frac{Y-E(Y)}{\sigma}\right)^3]$	W9	$N[Peaks(Ryy)]$	W12	$\frac{W11}{\frac{1}{L}\sum_{l=1}^{L} \lvert R_{yy}(l)\rvert}$
$cD_n(x)$: Detailed wavelet coefficients level of n $Y = cD_1(x), \dots, cD_3(x)$ R_{yy} : *Auto correlation function*					

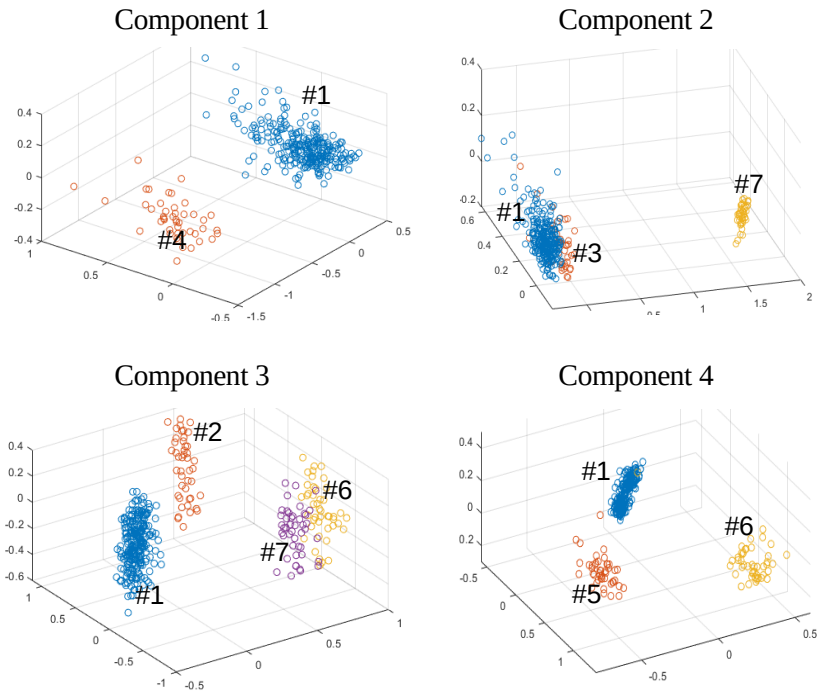

Figure 5. Dimensionality reduction using PCA. Features extracted from structure component 1-4 were reduced into 3 dimensions.

CONCLUSION AND FUTURE WORK

In this study, we proposed a method for real-time measurement of structural displacement and their application. We used phase-based optical flow with an optimized filter and parallel computing programming to create a system that can efficiently measure displacement in real-time. Furthermore, we validated the feasibility of the proposed method in condition monitoring through lab-scale experiments, demonstrating its potential application in data driven-based condition monitoring . Future plans include conducting research on the application of fast deep learning models for real-world applications .

ACKNOWLEDGEMENTS

This research was supported by the Korea Institute of Energy Technology Evaluation and Planning(KETEP) grant funded by the Korea government (MOTIE) (20203040040010, Development of commercial-ization technology on fault prediction and safety management for hydrogen refueling stations)

REFERENCE

1. Y. Xu, J.M.W. Brownjohn. 2018. “Review of machine-vision based methodologies for displacement measurement in civil structures”, J. Civ. Struct. Heal. Monit. 8 91–110.
2. J. Baqersad, P. Poozesh, C. Niezrecki, P. Avitabile. 2017. “Photogrammetry and optical methods in structural dynamics – A review”. Mech. Syst. Signal Process. 86, 17–34.
3. D. Lecompte, A. Smits, S. Bossuyt, H. Sol, J. Vantomme, D. Van Hemelrijck, A.M. Habraken. 2006. “Quality assessment of speckle patterns for digital image correlation”, Opt. Lasers Eng. 44.
4. W.H. Peters, W.F. Ranson, M.A. Sutton, T.C. Chu, J. Anderson. 1983. “Application Of Digital Correlation Methods To Rigid Body Mechanics”. Opt. Eng. 22.
5. S. Patsias, W.J. Staszewski. 2002. “Damage detection using optical measurements and wavelets”. Struct. Heal. Monit. 1, 5–22
6. N. Wadhwa, M. Rubinstein, F. Durand, W.T. Freeman. 2013. “Phase-based video motion processing”. ACM Trans. Graph. 32
7. M. Eitner, B. Miller, J. Sirohi, C. Tinney. 2020. “Effect of broad-band phase-based motion magnification on modal parameter estimation”. Mech. Syst. Signal Process. 146
8. A.J. Molina-Viedma, L. Felipe-Sesé, E. López-Alba, F.A. Díaz. 2018. “3D mode shapes characterisation using phase-based motion magnification in large structures using stereoscopic DIC”. Mech. Syst. Signal Process. 108. 140–155.
9. N.A. Valente, C.T. do Cabo, Z. Mao, C. Niezrecki. 2022. “Quantification of phase-based magnified motion using image enhancement and optical flow techniques”. Meas. J. Int. Meas. Confed. 189.
10. T. Gautama, M.M. Van Hulle. 2002. “A phase-based approach to the estimation of the optical flow field using spatial filtering”. IEEE Trans. Neural Networks. 13. 1127–1136.
11. Yinan Miao, Jun Young Jeon, Yeseul Kong, Gyuhae Park. 2022. “Phase-based displacement measurement on a straight edge using an optimal complex Gabor filter”. Mechanical Systems and Signal Processing, Volume 164.
12. Yinan Miao, Yeseul Kong, Jun Young Jeon, Hyeonwoo Nam, Gyuhae Park. 2023."A novel marker for robust and accurate phase-based 2D motion estimation from noisy image data".Mechanical Systems and Signal Processing. Volume 187.
13. HongZhang, Da-Fang Zhang,and Xia-An Bi. 2012. “Comparison and Analysis of GPGPU and Parallel Computing on Multi-Core CPU”, International Journal of Information and Education Technology, Vol. 2, No. 2